

NUMERICAL SIMULATIONS OF MAGNETICALLY CONFINED PLASMAS

A. Galatà*, C. S. Gallo, INFN-Laboratori Nazionali di Legnaro, (Padova), Italy
D. Mascali, G. Torrioni, INFN-Laboratori Nazionali del Sud, Catania, Italy

Abstract

Since 2012, the INFN ion source group has been undertaking an intense activity on numerical modelling of magnetically confined plasmas, presently carried out in the framework of the PANDORA project. The aim is the development of a predictive tool for the design of Electron Cyclotron Resonance (ECR) Ion Sources or Traps and ECR-based Charge Breeders, able to determine spatial density and energy distributions for both electrons and ions. The work mainly concerns the study of two aspects: on one hand, the interaction of an ion beam with a magnetized plasma; on the other hand, the microwave-to-plasma coupling, including the 3D plasma electrons dynamics in the confinement magnetic field and intra-particles collisions. This contribution describes the state-of-the-art of the work on both fronts: an overview of the beam-plasma interaction, the latest results about the ECR-plasma density fine structure, as well as electrons spatial temperature distribution will be shown.

INTRODUCTION

For the last years, the INFN ion source group has been focusing its research activity on the PANDORA (Plasmas for Astrophysics, Nuclear Decays Observation and Radiation for Archaeometry) project [1]. Its aim is a feasibility study of a new facility based on a state-of-the-art plasma trap confining extremely energetic plasma, to perform interdisciplinary research in the fields of nuclear astrophysics, astrophysics, plasma physics and applications in material science and archeometry. The plasma will become the environment for measuring, for the first time, nuclear decays rates in stellar-like conditions, in particular for ${}^7\text{Be}$, as a function of the in-plasma ionization state. These studies are of paramount importance for addressing several astrophysical issues in both stellar and primordial nucleosynthesis environment (e.g. determination of solar neutrino flux and ${}^7\text{Li}$ Cosmological Problem). The design of the trap, and in particular its magnetic field, will be based on the "B-minimum" geometry typical of Electron Cyclotron Resonance (ECR) ion sources [2]: in such machines, a dense and hot plasma, made of multicharged ions immersed in a dense cloud of energetic electrons, is confined by multi-Tesla magnetic fields and resonantly heated by some kW of microwave power in the 2.45–28 GHz frequency range. ${}^7\text{Be}$ will be injected inside the trap as a 1+ beam, using the well known ECR-based charge breeding technique [3], while its decay to ${}^7\text{Li}$ through electron capture will be tagged by detecting the 478 keV γ -ray emitted by the transition of ${}^7\text{Li}$ from the excited to the ground state (10% of branching ratio). In this framework,

the efforts are mainly dedicated to two fundamental aspects: on one hand, the development of a complete plasma diagnostic set-up able to detect plasma emission from the visible range to X-ray, in order to obtain spatially resolved ions and electrons density, as well as electrons temperature. Part of this work is presently carried out in collaboration with the Hungarian laboratory ATOMKI [4]. On the other hand, the development of an innovative numerical tool able to describe the interaction of the injected beam with the confined plasma, and also predict the plasma density and temperature fine structure, so as to maximize the injection and subsequent capture of the radioactive ions inside the trap. The paper will describe the state-of-the-art of the work on this last aspect: the results of the simulations of the beam-plasma interaction will be shown first, followed by the progresses made towards a plasma self-consistent description in terms of electrons density and temperature.

THE BEAM-PLASMA INTERACTION

A mentioned before, radioactive species will be injected in the PANDORA trap by employing the charge breeding technique, widely used in Isotope Separation On Line (ISOL) facilities whose aim is the post-acceleration of radioactive ions for nuclear physics experiments. As in the case of the SPES project, under construction at INFN-LNL [5], the charge breeding within PANDORA will be ECR-based: with this technique, the radioactive species produced in the so-called target-ion source-system are extracted as a 1+ beam from dedicated sources, transported along electrostatic beam lines, decelerated to very low energies (in the eV range), and then injected into the Charge Breeder. Once inside the plasma, radioactive 1+ ions suffer a huge number of small angle elastic ion-ion collisions (the so-called Spitzer collisions [6]) that eventually lead to thermalization with plasma ions, and are then extracted as a highly charged ion beam after charge multiplication through step-by-step ionizations by energetic electrons. The INFN ion source group developed an innovative fully 3D numerical approach in a MatLab environment, able to reproduce the beam-plasma interaction and its subsequent ionization [7]. The code implements a formalism based on the Langevin equation [8] to describe the Spitzer collisions, while ionizations are calculated by using the Lotz formula [9] and included with a MonteCarlo approach. The validity of the code was demonstrated by reproducing two experimental results obtained with the PHOENIX Charge Breeder at the Laboratoire de Physique et de Cosmologie, by injecting sodium [10] and rubidium ions [7]. It also revealed to be very useful in understanding the influence of the injected beam parameters on the capture process, in particular the

* alessio.galata@lnl.infn.it

beam emittance and energy spread [11]. The plasma was implemented following the plasmoid/halo scheme [12]: the numerical analysis carried out regarded the effect of different plasma parameters on the capture process, in particular the plasma density and ion temperature (electrons are involved only in the ionization process). An example is given in Fig. 1, showing the percentage of particles losses as a function of the injection energy for different plasma densities and an ion temperature $KT_i=0.5$ eV, by injecting $^{85}\text{Rb}^{1+}$ ions produced by a surface ionization source (see ref. [7]).

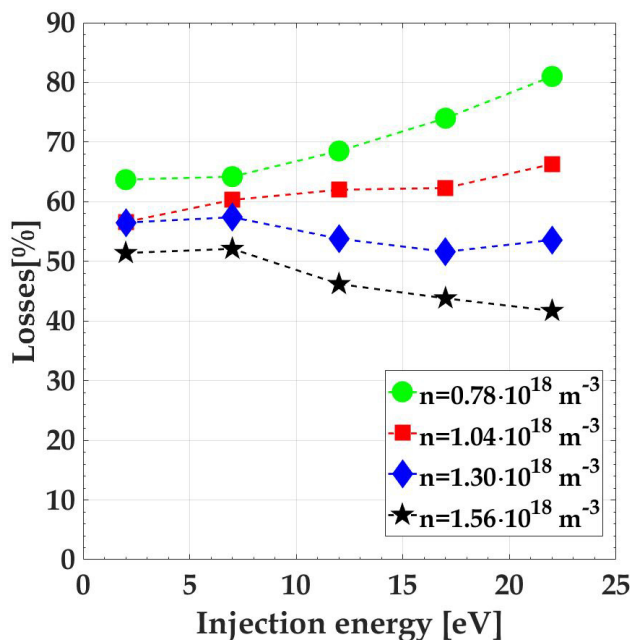


Figure 1: $^{85}\text{Rb}^{1+}$ ions losses as a function of the injection energy for different simulated plasma densities and an ion temperature $KT_i=0.5$ eV.

As expected, ions losses increase by decreasing the plasma density but their trends as a function of the injection energy change going from the highest to the lowest. For the highest one (close to the cut-off for the Charge Breeder's operating frequency of 14.521 GHz), in fact, losses decrease with energy because the friction and diffusion effects prevents injected ions to enter deep inside the plasma for low velocities. On the contrary, for the lowest density the minimum losses appear for the lowest injection energy and then increase steadily: in this case, it is easier for the injected ions to penetrate the plasma at low velocities, but as soon as the energy increases its slowing down capability becomes more and more ineffective. This effect is even clearer by looking at Fig. 2 that shows the ions losses as a function of the injection energy, respectively, in radial direction (radial losses), back to the injection side (axial losses), towards the extraction end plate (extraction losses) and through the 7 mm diameter extraction hole of the Charge Breeder (extracted), for the highest (bottom) and the lowest (top) density.

Following the interpretation above argued, for the highest density and the lowest energy most of the ions are lost from

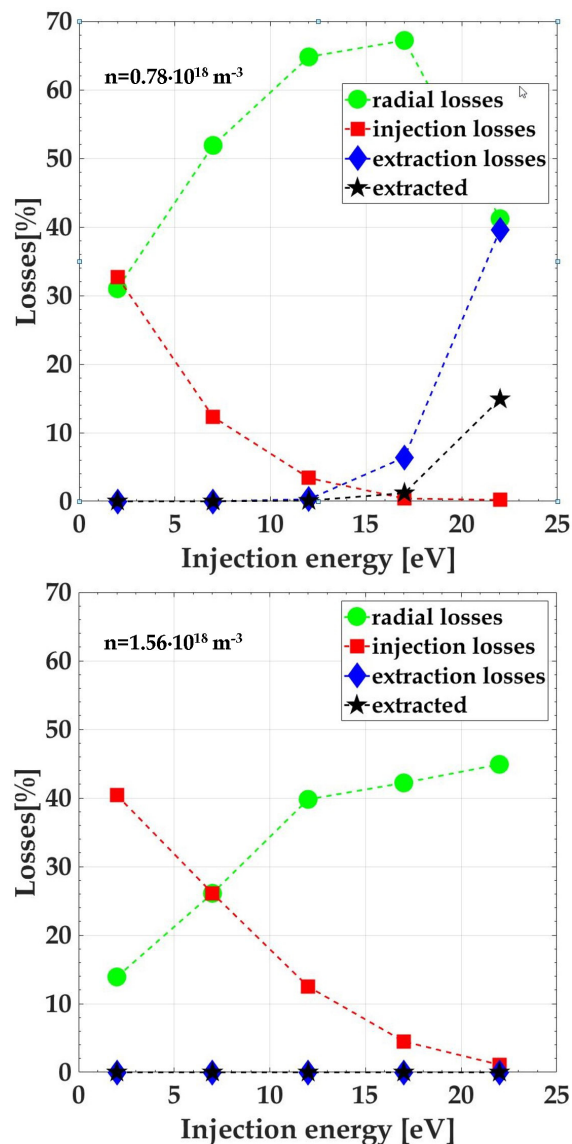


Figure 2: $^{85}\text{Rb}^{1+}$ ions losses in different directions as a function of the injection energy for $KT_i=0.5$ eV, $n=1.56\cdot 10^{18}$ m^{-3} (bottom) and $n=0.78\cdot 10^{18}$ m^{-3} (top). The directions considered are radial (green), back to the injection side (red), towards the extraction end plate (blue) and the one passing through the 7 mm diameter extraction hole of the Charge Breeder (extracted).

the injection side, while radial losses are limited and extraction losses negligible. When the energy increases, losses become mostly radial (increasing steadily) but even at the highest energy extraction losses are not observed. On the contrary, for the lowest density and energy, losses are shared between radial and axial direction: by increasing the energy, injection losses decrease faster than the previous case, while radial losses increase up to a maximum and then decrease due to the simultaneous increase of extraction losses. Some ions come out through the extraction hole, as very often observed experimentally.

Content from this work may be used under the terms of the CC BY 3.0 licence (© 2018). Any distribution of this work must maintain attribution to the author(s), title of the work, publisher, and DOI.

The numerical investigation led to the definition of a complete set of beam and plasma parameters able to reproduce experimental results with $^{85}\text{Rb}^{1+}$ ions, as described in ref. [7]: in particular, for the former an injection energy of 7 eV and an energy spread of 2 eV (typical of surface ionization sources); for the latter a plasmoid density $n=1.95 \cdot 10^{17} \text{ m}^{-3}$ and an ion temperature $KT_i=0.3 \text{ eV}$. This last parameter revealed to be very critical for an optimum capture of the injected ions. Very interesting information come from the ballistic of the process: Fig. 3 plots the injected particles trajectories at different time steps. As soon as particles approach the plasmoid, we can observe a spatial spread of the injected particles due to the fact that the energy spread is comparable to the injection energy, while once particles cross the resonance surface most of them remain trapped inside the plasmoid and very few are able to escape it. To detect the X-ray coming out from the plasma of the PANDORA trap with a precise spatial resolution, directly linked to the electrons energetic content, it is important to know the electrons loss paths along the magnetic field lines, because the strong bremsstrahlung emission due to their interaction with the plasma chamber walls could contaminate the measurement. Ambipolar diffusion forces ions and electrons to escape the trap following the same paths, so this information can be obtained also by following ions trajectories. Thanks to a specific routine included in the developed numerical code, it is able to store the positions of ions losses on the plasma chamber walls: Fig. 4 shows such positions in the case of ^{85}Rb ions. The two three-folded "stars" impressed to the plasma by the hexapolar field are clearly visible on the injection and extraction sides, as well as the six stripes in off-poles positions. By pointing the detectors in the zone between two adjacent stripes the influence of the bremsstrahlung emission should be limited or eventually avoided.

ELECTRONS DYNAMICS

The results showed in the previous section were obtained by implementing a realistic, but simplified, plasma-target model. The plasmoid/halo scheme used, in fact, distinguishes between a dense core inside the resonance surface and a rarefied halo outside, but in both zones the ions/electrons density and electrons temperature (at least the warm component, responsible for the ionizing collisions) are supposed to be uniform. In reality this is not the case, and in view of an efficient spatially resolved diagnostics within PANDORA the knowledge of the plasma fine structure is mandatory. Strong efforts have been making to obtain a self-consistent ECR-plasma description, by joining precise electromagnetic calculations, carried out with COMSOL multiphysics, with the electrons dynamics calculated with MatLab. In fact, on one hand in magnetized plasmas excited by microwaves (as is the case of ECR sources and traps) the electromagnetic field set-up inside the plasma chamber determines, through a resonant interaction, the energetic content of electrons and then the plasma density. On the other hand, the plasma is an anisotropic and dispersive medium

characterized by a 3D dielectric tensor, that must be taken into account for the calculation of the electromagnetic field in a kind of self-consistent loop. The approach is being followed consists of different steps: the first starts with the calculation of the electromagnetic field of the empty plasma chamber. Then, this field is used to calculate the dynamics of electrons generated uniformly inside the plasma chamber, by using a MatLab code derived directly from the one developed for ions, including relativistic effects. The code follows the evolution of N electrons until they escape the domain of simulation: at this stage particles dynamics is determined only by electromagnetic and magnetostatic fields. By using an ad-hoc routine, the code stores particles positions at each time step in a 3D matrix reflecting the domain of the simulation divided in cells of 1 mm^3 , creating an "occupation" map. This map is then scaled as it would be equivalent to a uniform density of $2 \cdot 10^{17} \text{ m}^{-3}$, obtaining a density map; this calculation concludes the first step. The density map is used to calculate the value of the plasma dielectric constant in each cell: the second step starts with new electromagnetic calculations, this time including a plasma (through its dielectric constant) distributed like the density map, following the approach used in [13]. Electrons dynamics is calculated again with the magnetostatic and the new electromagnetic field, creating this time not only an occupation (and so a density) map but also an energy map, obtained storing at each time step the energy of the electrons in another 3D matrix. By dividing the energy map to the occupation map, the spatial distribution of the average energy is obtained: by supposing it belongs to electrons with a Maxwell-Boltzmann distribution, a spatial temperature map can be derived by multiplying the average energy for the factor $(3/8)\pi$. With the temperature and density matrices, electrons dynamics is calculated again including this time the presence of the plasma, that is including the electron-electron collisions. Finally, the step is concluded with a new density map that can be used to calculate again the 3D dielectric tensor and then the electromagnetic field: this second step is repeated until the results show self-consistency, that is until the results from consecutive steps show negligible differences in the density and temperature matrices.

The work on this kind of approach is presently ongoing, but the preliminary results are already remarkable: Fig. 5 show the projection on the xy plane (left) and the radial profile along the x axis in the midplane (right) of the density map obtained after the second step, that is including the plasma in the electrons dynamics only one time. The electromagnetic power simulated is 100 W, while the geometry and the confining magnetic field are the same as in ref. [7]. It can be clearly observed that, even if electrons starts uniformly distributed inside the plasma chamber in the first step, at the end of the second one not only the plasmoid/halo structure is automatically formed, but also the fine structure of the plasmoid is clearly visible, a result never obtained with any previous numerical simulation. The plasma concentrates in a region around the axis, with a peak density around $3 \cdot 10^{17} \text{ m}^{-3}$, and its density drops of about one order of magnitude

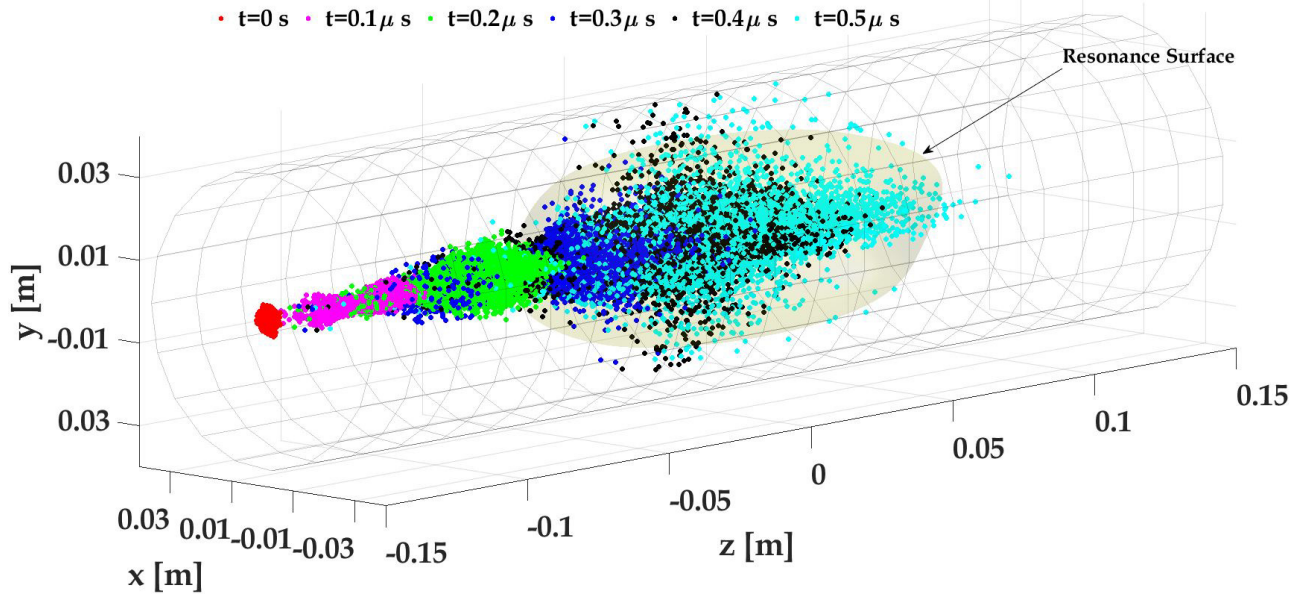


Figure 3: Plot of the injected particles trajectories at different time steps for an injection energy of 7 eV: $t=0 \mu\text{s}$ (red), $t=0.1 \mu\text{s}$ (magenta), $t=0.2 \mu\text{s}$ (green), $t=0.3 \mu\text{s}$ (blue), $t=0.4 \mu\text{s}$ (black), $t=0.5 \mu\text{s}$ (cyan). The cylinder represents the Charge Breeder plasma chamber, while the egg-shaped surface indicates the resonance surface containing the plasmoid.

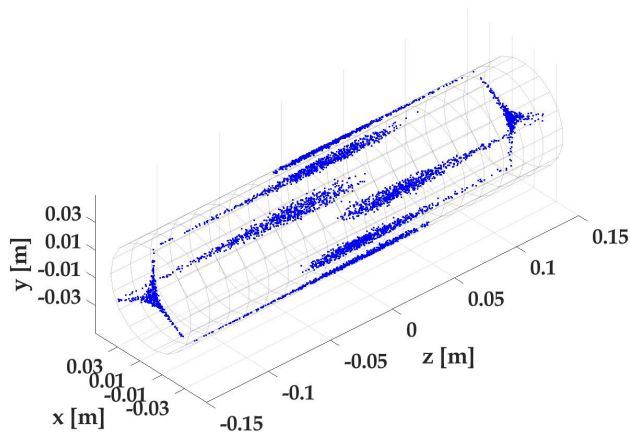


Figure 4: Location of $^{85}\text{Rb}^{1+}$ losses on the plasma chamber walls; the cylinder represents the Charge Breeder plasma chamber.

within the plasmoid, as shown by the radial profile. The results gave also for the first time a picture of the electron temperature distribution: Fig. 6 shows on the top the xz projection of the temperature map. The electrons temperature is not uniform inside the plasmoid but "hot-spots" in the keV appear in different zones: plotting the isosurface of those hot-spots in the bottom part Fig. 6 it is clear that those zone are localized all around the resonance surface, where electrons gain energy interacting with the electromagnetic field. These last results are unprecedented and make the developed numerical code a unique tool for the description of magnetically confined plasma typical of ECR ion sources and traps.

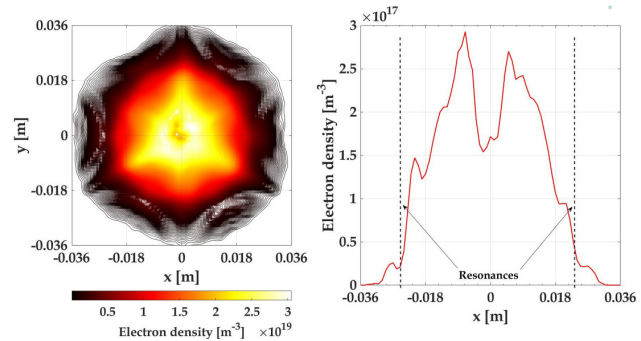


Figure 5: Density plots obtained after two steps of the self-consistent loop: projection on the xy plane (left) and radial profile along the x axis in the midplane (right).

CONCLUSIONS AND PERSPECTIVES

The results shown in this paper confirm the validity of the numerical code developed by the INFN ion source group in describing the beam-plasma interaction: Figs. 1–4, together with those shown in ref. [7,10,11], demonstrate its capability in simulating properly the slowing down and capture of the injected ions for light and heavy species, identifying the beam and plasma parameters playing a key role in the process. The preliminary results of the electrons dynamics show for the first time ever that the ECR plasma automatically assume a plasmoid/halo structure, with a peculiar distribution of density and temperature in the plasmoid. In the next future the efforts will be concentrated in obtaining a self-consistent description of electrons behaviour inside the plasma and the spatially resolved ions charge state distribution, with the aim at developing a complete predictive

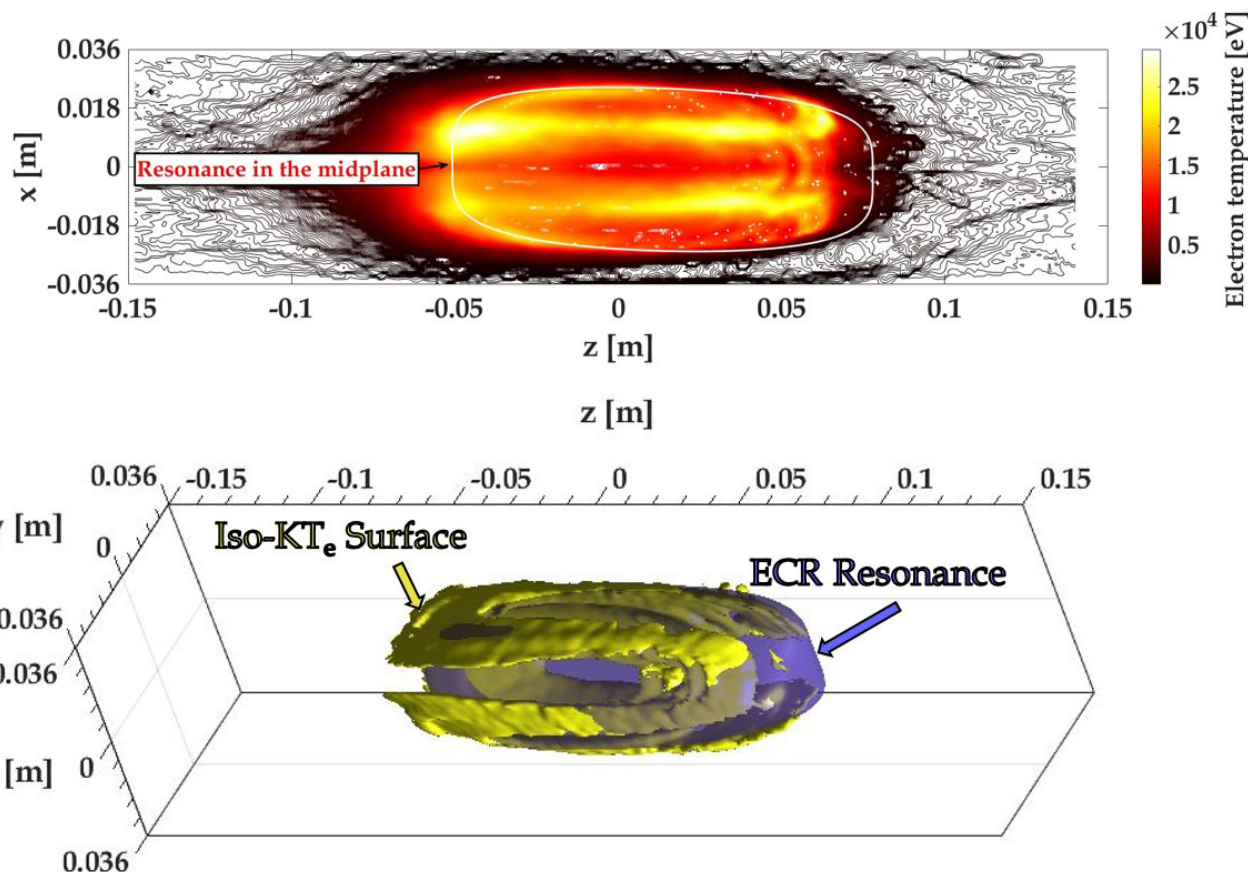


Figure 6: Electrons temperature spatial distribution: projection on the xz plane (up) and isosurface (down). The isosurface shows the points where the temperature has the highest values; the resonance surface is visible in blue.

numerical tool for the design of new ECR ion sources and traps and ECR-based Charge Breeders, in particular in the framework of the PANDORA project.

REFERENCES

- [1] D. Mascali *et al.*, "PANDORA, a new facility for interdisciplinary in plasma physics", *Eur. Phys. J. A*, vol. 53 p. 145, (2017).
- [2] R. Geller, *Electron cyclotron resonance ion sources and ECR plasmas*, Bristol: IOP (1996).
- [3] N. Chauvin *et al.*, "The $1^+ \rightarrow n^+$ charge breeding method for the production of radioactive and stable continuous /pulsed multi-charged ion beams", in *Proceedings of the 14th International Workshop on ECR Ion Sources*, CERN, Geneva, Switzerland, 3–6 May 1999.
- [4] R. Racz *et al.*, *Electron cyclotron resonance ion source plasma characterization by energy dispersive X-ray imaging*, *Plasma Sources Sci. Technol.* **26** (2017) 075011.
- [5] A. Galatà *et al.*, "ADIGE: the radioactive ion beam injector of the SPES project", *J. Phys.: Conf. Ser.*, vol. 874, p. 012052, (2017).
- [6] L. Spitzer Jr, "Physics of Fully Ionized Gases", *Dover Publications, Inc., Mineola, New York* (2006).
- [7] A. Galatà *et al.*, "A three-dimensional numerical modelling of the PHOENIX-SPES charge breeder based on the Langevin formalism", *Rev. Sci. Instrum.*, vol. 87, p. 02B507, (2016).
- [8] W. M. Manheimer *et al.*, "Langevin Representation of Coulomb Collisions in PIC Simulations", *J. Comput. Phys.* vol. 138, p.563, (1997).
- [9] W. Lotz, "An empirical formula for the electron-impact ionization cross-section", *Z. Phys.*, vol. 206, p. 205, (1967).
- [10] O. Tarvainen *et al.*, "Diagnostics of a charge breeder electron cyclotron resonance ion source helium plasma with the injection of $^{23}\text{Na}^{1+}$ ions", *Phys. Rev. Accel. Beams*, vol. 19, p. 053402, (2016).
- [11] A. Galatà *et al.*, "Influence of the injected beam parameters on the capture efficiency of an electron cyclotron resonance based charge breeder", *Phys. Rev. Accel. Beams*, vol. 20, p. 063401, (2017).
- [12] A. A. Ivanov and K. Wiesemann, "Ion confinement in electron cyclotron resonance ion sources (ECRIS): importance of nonlinear plasma-wave interaction", *IEEE Trans. Plasma Sci.*, vol. 33, p. 1743, (2005).
- [13] A. Galatà *et al.*, "Electromagnetic analysis of the plasma chamber of an ECR-based charge breeder", *Rev. Sci. Instrum.*, vol. 87, p. 02B505, (2016).